



Contents lists available at ScienceDirect

Computers in Biology and Medicine

journal homepage: www.elsevier.com/locate/cbm

Computational classification of different wild-type zebrafish strains based on their variation in light-induced locomotor response

Yuan Gao^{a,1}, Gaonan Zhang^{b,1}, Beth Jelfs^a, Robert Carmer^{a,c}, Prahatha Venkatraman^b, Mohammad Ghadami^a, Skye A. Brown^b, Chi Pui Pang^d, Yuk Fai Leung^{b,e,*}, Rosa H.M. Chan^{a,**}, Mingzhi Zhang^{f,***}

^a Department of Electronic Engineering, City University of Hong Kong, Tat Chee Avenue, Kowloon, Hong Kong

^b Department of Biological Sciences, Purdue University, 915W. State Street, West Lafayette, IN 47907, USA

^c Department of Statistics, Purdue University, 250N. University Street, West Lafayette, IN 47907, USA

^d Department of Ophthalmology and Visual Sciences, Chinese University of Hong Kong, Hong Kong

^e Department of Biochemistry and Molecular Biology, Indiana University School of Medicine—Lafayette, 625 Harrison Street, West Lafayette, IN 47907, USA

^f Joint Shantou International Eye Center, Shantou University & the Chinese University of Hong Kong, Shantou, China

ARTICLE INFO

Article history:

Received 8 June 2015

Accepted 18 November 2015

Keywords:

Zebrafish

Computational classification

Light-induced locomotor response

Visual motor response

Support vector machines

ABSTRACT

Zebrafish larvae display a rapid and characteristic swimming behaviour after abrupt light onset or offset. This light-induced locomotor response (LLR) has been widely used for behavioural research and drug screening. However, the locomotor responses have long been shown to be different between different wild-type (WT) strains. Thus, it is critical to define the differences in the WT LLR to facilitate accurate interpretation of behavioural data. In this investigation, we used support vector machine (SVM) models to classify LLR data collected from three WT strains: AB, TL and TLAB (a hybrid of AB and TL), during early embryogenesis, from 3 to 9 days post-fertilisation (dpf). We analysed both the complete dataset and a subset of the data during the first 30 s after light change. This initial period of activity is substantially driven by vision, and is also known as the visual motor response (VMR). The analyses have resulted in three major conclusions: First, the LLR is different between the three WT strains, and at different developmental stages. Second, the distinguishable information in the VMR is comparable to, if not better than, the full dataset for classification purposes. Third, the distinguishable information of WT strains in the light-onset response differs from that in the light-offset response. While the classification accuracies were higher for the light-offset than light-onset response when using the complete LLR dataset, a reverse trend was observed when using a shorter VMR dataset. Together, our results indicate that one should use caution when extrapolating interpretations of LLR/VMR obtained from one WT strain to another.

© 2015 Published by Elsevier Ltd.

1. Introduction

Over the last two decades, the zebrafish has been increasingly used to study human diseases due to its genetic similarities with humans [1,2]. In recent years, the zebrafish has also been used in high-throughput behavioural studies in various fields, including but not limited to, neurobiology [3–8], pharmacology [6,9] and toxicology [10–14]. This ever increasing popularity is driven by

several desirable properties of the zebrafish model, in particular high fecundity which allows for a large number of embryos to be simultaneously tested [15].

It should, however, be noted that different wild-type (WT) strains differ in their genetics [16,17] which can result in differences in their behaviour [13,18,19]. For example, researchers have found that different WT strains vary in their locomotor and shoaling behaviour at different developmental stages. Variations in the development of both behaviours have been reported between AB² and TU³ larvae. At the onset of locomotor behaviour, the TU larvae have been observed as having a wider range of activity when compared to AB larvae [19]. In addition, these

* Corresponding author at: Department of Biological Sciences, Purdue University, 915 W. State Street, West Lafayette, IN 47907, USA.

** Corresponding author.

*** Corresponding author.

E-mail addresses: yfleon@purdue.edu (Y.F. Leung),

rosachan@cityu.edu.hk (R.H.M. Chan), zmz@jsiec.org (M. Zhang).

¹ These authors have equal contribution.

<http://dx.doi.org/10.1016/j.compbiomed.2015.11.012>

0010-4825/© 2015 Published by Elsevier Ltd.

² <http://zfin.org/action/genotype/genotype-detail?zdbID=ZDB-GENO-960809-7>

³ <http://zfin.org/action/genotype/genotype-detail?zdbID=ZDB-GENO-990623-3>

strains have different rate in maturation of shoaling behaviour. This variation has been attributed to the difference in neurotransmitter levels in the brains of these lines during development [20]. AB larvae have also been shown to differ from TL larvae, exhibiting greater activity in the dark at 5 and 6 days post-fertilisation (dpf), and lower activity in both light and dark at 7 dpf than the TL larvae [13].

It is worth considering that these metrics have also been observed to vary within the same WT strain. The study by Lange and colleagues for example showed that not only the EK⁴, TU and WIK⁵, but also, interestingly, the two AB lines from different labs differed in their behaviour, such as the mean distance, speed and duration of swimming [18]. Since these lines were originally derived from the same founders, the large locomotor difference may be caused by genetic drift, or alternatively, fish locomotor behaviour can also be shaped by extrinsic factors. These factors can include the size of the containing well [21], as well as the time of day and light illumination levels [14]. With this in mind, considering all of the above results, it is critical to investigate the unique responses in a particular WT strain in the design and interpretation of behavioural studies.

A popular behavioural assay used in many of these studies is the light-induced locomotor response (LLR) [22]. Upon a drastic light onset or offset, zebrafish larvae display a visual startle response. This would give rise to a rapid and characteristic swimming behaviour that can be simultaneously measured across multiple larvae. Different variants of LLR have been used to study WT behaviour [13,18,19] and visual defects [12,15,22–24], and screen neuroactive drugs [6,9,11,12]. In these studies, two major methods were used to measure larval movement. One way is to compare the larval position from frame to frame [6,12,15,22–24]. If the change in position exceeded a pre-determined threshold, the larva would be considered moving between these two frames. Then, the larval activity over a period of time would be summarised as the duration of movement per unit time. Another popular way to measure larval movement is to track the individual displacement in the whole video [11,13,18,19,25,26]. Using this measurement, swimming speed and velocity, and speed of habituation of the larvae can be calculated. Despite the growing popularity of the LLR assay, it still remains unclear whether the initial short phase (first few seconds) of the LLR, i.e. the visual motor response (VMR) [23], would vary for different WT strains. The significance of this can be seen when considering the use of zebrafish to screen eye drugs. The VMR is known to be primarily driven by vision [23], while latter parts of the LLR are driven by both vision and non-ocular photoreceptors [26]. While the VMR in visual mutants has been studied [12,15,22–24], variations due to genetic differences in WT strains are less clear. Many studies have investigated LLR data by summarizing activity data into bins of a minute or more in duration, so as to capture long-term behavioural changes [11,13,14,18,19,21,25,26]. Hence, the dynamics associated with the VMR changes, which occur in only the first few seconds, are not distinguishable from the rest of the data it has been grouped with. Of the few groups that have used the VMR to interpret results [12,15,23,27], none have analysed different WT strains.

The dynamical changes in zebrafish behaviour have recently been analysed by various machine learning methods. They are capable of identifying subtle differences which may be missed by manual analysis [6,9,22,32]. For example, HMM has been used to study the behavioural change in zebrafish under chemical stress according to pre-defined behavioural patterns [29,30].

Furthermore, hierarchical clustering has been used for drug screening using zebrafish model, in which small molecules with similar pharmacological activity were clustered based on similarity in resulting behaviours of treated zebrafish [6]. Support vector machine (SVM) has been used to categorize the episodes of movement for zebrafish into several maneuvers, including slow forward swim, routine turn, and escape. [31]. SVM has also been used to develop a phenotype recognition model for toxicity screening with zebrafish embryo [32]. Recently, we have also used SVM to distinguish WT and mutant zebrafish by their different responses to the light-stimuli [22]. These studies strongly demonstrate the utility of machine-learning methods for analysing the dynamical changes in zebrafish behaviour under chemical stresses and genetic mutations.

Nonetheless, these studies utilised zebrafish with the same strain/background. As indicated before, the strain difference may affect resulting zebrafish behaviour and subsequent data analysis. Thus, it is critical to conduct a control study of the WT zebrafish dynamical changes using machine-learning methods, to facilitate their use in dynamical analysis of zebrafish behaviour. In this paper, we used machine learning techniques to study the difference in the VMR and LLR between various WT strains from 3 to 9 dpf. The contribution of our work is threefold: First, our study has demonstrated that the inherent differences between the WT strains affect classification accuracy. Hence, it is critical to use matching WT strains as proper controls in machine-learning studies. Second, our study has revealed that different time lengths should be used to classify locomotor behaviour under light onset and light offset, so as to achieve the best accuracy. This information is critical for the field to design efficient assay scheme. Third, our results have also suggested that the distinguishable information of WT strains in the light-ON response differs from that in the light-OFF response. For example, when using the 30-min LLR, three WT strains displayed a larger difference under the light-OFF stimulus than under the light-ON stimulus. This difference again is critical for future studies that aim at using machine-learning methods to analyse similar behavioural responses.

2. Materials and methods

2.1. Zebrafish maintenance, breeding and embryo collection

In this study, three strains of WT zebrafish were used: AB, TL and TLAB⁶ (AB/TL: A hybrid of AB and TL). They were maintained, bred and the embryos collected according to standard procedures [33]. Specifically, the collected embryos were maintained in E3 medium at 28 °C in an incubator with the same light-dark cycle as in the fish facility. The medium was changed every day and unhealthy embryos were discarded. At 3 dpf, healthy embryos were further selected based on the following criteria: no visible physical defects such as bent spines, bloated bodies or other deformities. These healthy embryos were transferred to a 96-well plate for use in the subsequent behavioural assay. The health of these embryos was then inspected every day. During the inspection, embryos or larvae that showed any signs of abnormality during the course of behavioural experiment were excluded from the final data analysis. The numbers of animals used on each day are summarised in Table 1, which shows the number of health fish from two biological replicates with 96 embryos per run. All protocols were approved by the Purdue Animal Care and Use Committee.

⁴ <http://zfinfo.org/action/genotype/genotype-detail?zdbID=ZDB-GENO-990520-2>

⁵ <http://zfinfo.org/action/genotype/genotype-detail?zdbID=ZDB-GENO-010531-2>

⁶ <http://zfinfo.org/action/genotype/genotype-detail?zdbID=ZDB-GENO-031202-1>

Table 1
The sample size of each WT strain per dpf.

WT Strains	3 dpf	4 dpf	5 dpf	6 dpf	7 dpf	8 dpf	9 dpf
TLAB	188	185	190	185	183	182	190
TL	192	178	176	176	173	183	173
AB	192	192	192	191	189	188	186

2.2. Behavioural data analysis

The behavioural analysis can be broken down into three main components: data collection, feature extraction and classification [22]. An overview of these components is outlined here and the details of each component will be described in the next sections. The LLR data was collected and pre-processed by Zebrabox (Viewpoint Life Sciences, Lyons, France) to give the zebrafish movement in terms of the movement burst duration. After that, the behavioural data were represented by a set of features that have been specifically defined to describe the LLR and VMR data of zebrafish [6,22]. Then, these features were analysed by the classification algorithms to allocate the larval samples into distinct groups corresponding to different strains. Specifically, the algorithms utilised the numerical values obtained from the features as a descriptor of a specific larva to decide which strain best fit the observed behaviour of that larva. In an independent study, the same dataset was also used to establish a statistical framework for analysing similar behavioural data, and for evaluation of inherent variations of the experiments [34].

2.2.1. Behavioural data collection

All behavioural experiments were conducted inside an apparatus called Zebrabox (Viewpoint Life Sciences, Lyons, France), in which the larvae were plated in a 96-well plate, isolated from light from the environment, and stimulated by white light controlled by a light-controlling unit from the bottom of the plate. The larval movement was recorded by an infra-red camera under continuous infra-red light illumination, which the larvae could not perceive. With this setup, the behavioural data was collected based on Emran and colleagues' framework [23,27]. In brief, the larvae were placed in a 96-well plate inside the Zebrabox for 3.5 h of dark adaptation. During the assay, a bright white light stimulus with stable intensity at 1390.94 lx was shone in the following sequence: ON-OFF-ON-OFF-ON-OFF, each for a period of 30 min. The movement of the larvae was detected by an infra-red camera that captured video at a rate of 30 frames per second. Then, a movement metric (burst duration) was defined by the following method. Firstly, it is necessary to identify the active pixels that represent the movement of a larva in consecutive frames. This was achieved by setting a detection sensitivity threshold, such that, when the change in the grey level of a pixel between successive frames was greater than the detection sensitivity, the pixel was considered active. In this study, the detection sensitivity was set at 6 with the grey level ranging from 0 to 255. Following this, a burst threshold (BT) was set so that when the number of active pixels in consecutive frames were larger than the BT, the movement was defined a burst (i.e. a true movement regarded by our assay). In our analysis, we set BT=0 in order to utilise all the active pixels without filtering out any subtle differences between the strains. This approach provides the best classification performance as demonstrated in our previous study [22]. The data was then segmented into 1-s bins, for each bin the duration of the frame-to-frame movement (i.e. the bursts) is given as the burst duration, that is, the fraction of the 1 s bin that a larva moves. For the sequence of 6 repeated light-stimuli (ON-OFF-ON-OFF-ON-OFF),

we treat each ON-OFF sequence as one trial, and the three ON-OFF trials are averaged for further analysis.

The scheme described above was used to collect larval movement data from 3 to 9 dpf with the dark adaptation of all experiments starting at approximately 11 a.m. These developmental stages cover the period when the retina begins to differentiate and the initial visual behaviour first appears [35–37] to the last stage zebrafish can survive without feeding. For each WT line, two independent replicates were run using a full plate of 96 healthy embryos. The health of the embryos was inspected every day and half of the medium was replaced. Any embryos/larvae that showed gross morphological defects during the course of the experiments, such as inflated swim bladder or bent trunk vertebrae were excluded from the final data analysis.

2.2.2. Feature extraction and classification

In this work, we employ the feature set that we used previously [22], which implements a set of empirically selected biological metrics and is an extension of the method presented in [6]. This approach has been experimentally verified as an effective descriptor of zebrafish behaviour triggered by light ON/OFF, and can lead to better classification accuracy when compared with other methods such as Symbolic Aggregate approXimation (SAX) [38].

In order to quantify the amount of continuous movement of the zebrafish, we explicitly define two metrics: “active bout” and “rest bout”. An active bout is the number of consecutive bins in which the burst durations are larger than zero, with the opposite being regarded as a rest bout. The definitions of active/rest bout are illustrated in Fig. 1.

In the following, we extracted the lengths of the first active/rest bout, and the average lengths of all active/rest bouts as features. Specifically, the length of a bout is defined as the number of bins within that bout. We also used the mean of the total response (and active response) as features, which is the average of all the burst durations (and the average of only the positive burst durations) in the whole time-series dataset. In addition to the metrics describing the amount of activity, sample entropy is also used as a feature to quantify the randomness, or complexity, of the movement. Sample entropy is measure based on a conditional probability of the similarity between two sequences of data (please refer to Section S1.1. of supplementary material for details). This approach is commonly used to measure physiological time series [39,40]. The elements of the feature set used in this study are shown in Table 2.

Having defined the feature set, classification algorithms were implemented to distinguish different zebrafish strains. As our previous results showed that the support vector machine (SVM)

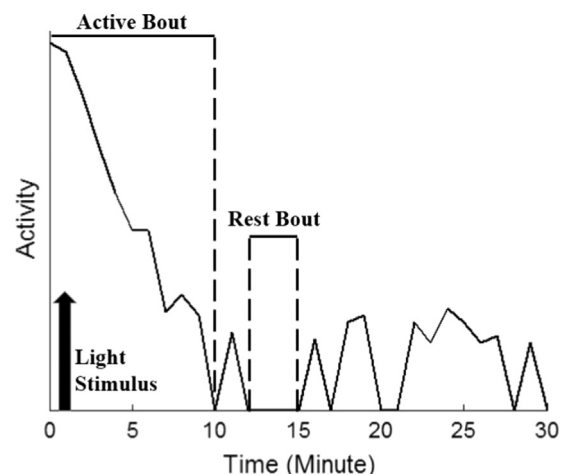


Fig. 1. The illustration of key features.

Table 2
Elements of feature set.

Maximal amplitude	Length of first active bout
Number of rest bouts	Length of first rest bout
Number of active bouts	Mean of the total response
Averaged rest bout length	Mean of the active response
Averaged active bout length	Sample entropy

classifier provided a more consistent classification of different zebrafish mutants [22], the results presented hereafter, used SVM to study the differences of zebrafish strains⁷. The results obtained from other classification methods are presented in Table S1 and S2 of the supplementary material, and support the choice of SVM as a superior method for classifying zebrafish locomotor behaviour.

In this work, we fixed the hyperparameters of SVM as the ones used in our previous research on the zebrafish classification [27]: the coefficient of slack variables was set to 2 and the kernel width was set to 0.125. To the best of our knowledge, fixing these hyperparameters is the most commonly-used way before training the model for the problem with a specific application. In this study, we have only one group of hyperparameters (i.e. one model), and we used this model for studying the difference between different zebrafish strains. Hence, there is no validation set for model selection.

To ensure that reliable results were obtained, cross validation was conducted. Cross validation is an approach for estimating the expected level of fit of the model to a data set (i.e. the validation set) that is independent of the data that are used to train the model (i.e. the training set). These validation and training datasets are partitioned several times from the whole data set for multiple trials, such that they are independent from and complementary with each other in each trial. The results of all trials will be averaged. In this study, we used 500 times 10-fold cross validation for each classification problem. That is, the dataset was randomly divided into 10 equal-sized complementary parts. For each trial, 9 parts were chosen for training, whereas the remaining 1 part was used for validation. This procedure was repeated until each of the 10 parts had been used exactly once as the validation data to give a 10-fold cross validation. Finally, this procedure was repeated 500 times to give 500 times 10-fold cross validation. This cross-validation procedure provided a useful estimator of model performance [42], because the mean accuracy estimated from multiple partitions of training and validation dataset better accounted for the data distribution of the whole dataset. In other words, it avoided the problem in single-partitioned data that the training and validation datasets might obey different data distributions [42].

In the following sections, we used classification accuracy as the metric to illustrate the results. The accuracy is defined by the following equation:

$$\text{accuracy} = \frac{\text{number of correctly classified samples}}{\text{total number of samples}} \times 100\%$$

3. Results

Fig. 2 shows the plot of mean burst duration for the TL, AB and TLAB strains at 3 dpf. This plot was chosen in order to give an intuitive representation of the difference in behaviour among zebrafish strains, since this is the stage when the retina matures and the initial visual behaviour can be detected [35–37]. For brevity, the remaining plots of burst duration at different stages of development are provided in the supplementary material

3.1. Evaluation of the differences between three WT strains by machine learning

The activity data (e.g., Fig. 2) were used for classification by SVM. Specifically, two time periods were used as input data: (1) the complete LLR dataset with 30 min for each light onset and offset (30-min LLR); and (2) the first 30 s of the LLR dataset after light change (first 30-s LLR). As this initial period of activity is substantially driven by vision, it is also known as the VMR. The overall classification accuracies utilising the 30 min-LLR and the first 30-s LLR (VMR) are summarised in Fig. 3. In both cases, light onset (light-ON) and light offset (light-OFF) data were incorporated into the SVM models. In terms of the two-class classification problems (i.e. TLAB vs. TL, TLAB vs. AB, TL vs. AB), the accuracies for TL vs. AB outperformed others in most cases, especially when using the first 30-s LLR (VMR) (the only exception is for 5-dpf data). Also, the highest accuracies for two-class problems, 86.0% (using the 30-min LLR) and 90.6% (using the first 30-s LLR [VMR]), were achieved when classifying TL and AB on 8-dpf data. Fig. 3 also shows that the accuracies of the 3-class problem (TLAB vs. TL vs. AB) were significantly lower. One interpretation is that although we could find a discriminative margin in SVM which distinguished TL from AB, this margin did not hold after adding the TLAB data. This is because TLAB is a hybrid of TL and AB and may share similar behavioural traits, therefore, TLAB's features were likely to appear within the margin and compromise the discriminatory power. As the TL and AB strains possessed the most significant difference, we focus the analysis on these two strains hereafter.

3.2. The effects of developmental change and different amounts of data on classification accuracy

The difference in the LLR of WT strains also varied with stage. Fig. 4 shows the classification accuracies of TL vs. AB using the 30-min LLR and the first 30-s LLR (VMR). Again, both light-ON and light-OFF data were incorporated into these SVM models. In both cases, the highest accuracies were achieved with 8-dpf data (i.e. 85.95% for the 30-min LLR and 90.61% for the first 30-s LLR [VMR]). For the classification using the 30-min LLR, the accuracies monotonically increased until 8 dpf. Whereas for classification using the first 30-s LLR (VMR), the accuracies following the initial increase, exhibited a drop in performance at 5 and 6 dpf before reaching its maximum at 8 dpf. In both classification cases, a slight decrease in accuracy was observed at 9 dpf. The results also showed that in most cases (3, 4, 7, 8, and 9 dpf), the accuracies using the first 30-s LLR (VMR) outperformed those using the 30-min LLR, suggesting that TL and AB have a larger difference in their first 30-s LLR (VMR).

3.3. The difference in classification accuracy between the light-ON and light-OFF responses

In order to investigate the difference in LLR when using the light-ON stimulus compared to the light-OFF stimulus, we conducted classification studies with the features extracted from each stimulus separately. Fig. 5 shows the classification accuracy for TL vs. AB during light-ON period or light-OFF period using the 30-min LLR (left sub-figure) and the first 30-s LLR (VMR) (right sub-figure). The classification accuracies in both cases were generally lower than those when both light-ON and light-OFF data were combined (Fig. 4). Further, the results show that the classification accuracies were higher during the light-OFF stimulus than the light-ON stimulus in the 30-min LLR (Fig. 5, left sub-figure). This observation is consistent with that revealed by the mean plots of Burst Duration against time (Fig. S1–S7 of the Supplementary

⁷ An open source C++ library LIBSVM [41] was used for the analysis.

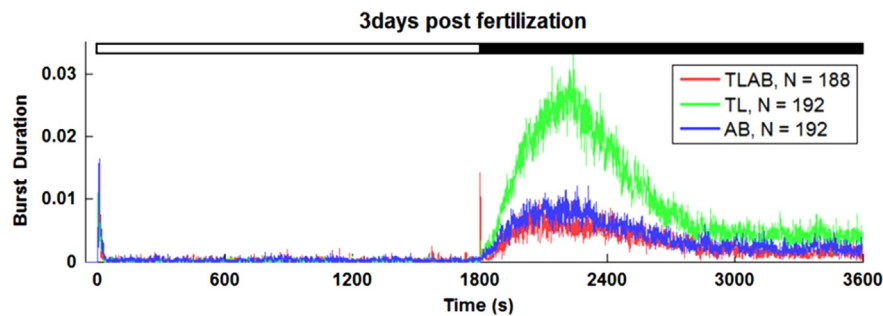


Fig. 2. Plot of mean burst duration for three WT strains at 3 dpf. This plot shows the averaged burst duration of three WT strains: TLAB (red trace), TL (green trace), and AB (blue trace) at 3 dpf. The first and last 1800 s (30 min) represent the averaged response of three repeats of the ON-OFF stimulus sequence, respectively. The ON and OFF stimuli are indicated by the white and black bars at the top. The total number of larvae is indicated in the inset. (For interpretation of the references to colour in this figure legend, the reader is referred to the web version of this article.)

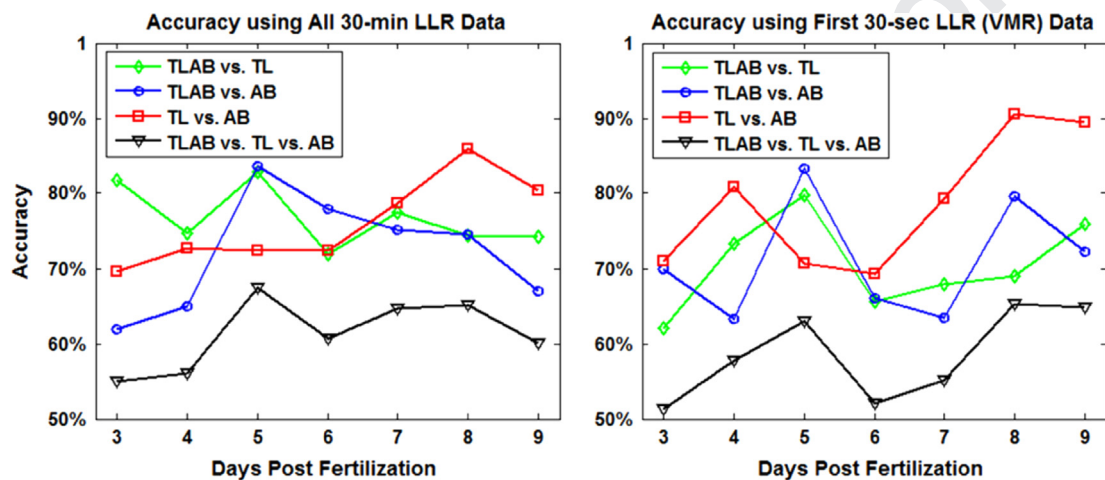


Fig. 3. Classification accuracy for different WT zebrafish strains from 3 to 9 dpf using LLR data of different lengths. The left figure shows the classification results using the 30-min LLR, while the right figure shows the results using the 30-s LLR (VMR). In each figure, there are four line plots indicating the classification accuracies for TLAB vs. TL (green), TLAB vs. AB (blue), TL vs. AB (red), and TLAB vs. TL vs. AB (black) respectively. These line plots are the average of the 500 times 10-fold cross validation. Data from both light-ON and light-OFF stimuli were used in this analysis. (For interpretation of the references to colour in this figure legend, the reader is referred to the web version of this article.)

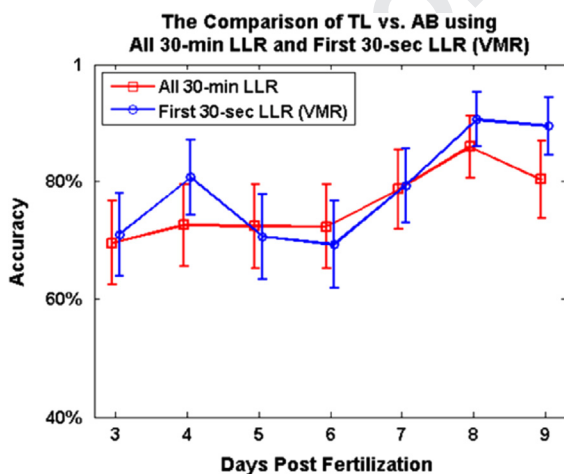


Fig. 4. Classification accuracies for TL vs. AB from 3 to 9 dpf using LLR data of different lengths. In this plot, the classification was conducted using data either from the 30-min LLR (red) or the first 30-s LLR (VMR) (blue). The activity from both light-ON and light-OFF stimuli were used in the analysis. The line plots and the error bars indicate the mean and the standard deviation of the 500 times 10-fold cross validation. (For interpretation of the references to colour in this figure legend, the reader is referred to the web version of this article.)

Material). Over the whole 30-min duration of light-OFF stimulus, the larvae were more active. This higher activity should provide more discriminative features, such as Number of Active/Rest Bout, and Sample Entropy for classification.

Conversely, in the first 30-s LLR (VMR), the classification accuracies were higher during the light-ON stimulus than the light-OFF stimulus (Fig. 5, right sub-figure). The most significant difference in accuracies between the light-ON and light-OFF stimuli was seen at 3 and 4 dpf. This observation is also consistent with the lack of activity in the light-OFF mean plots compared with the light-ON ones for TL and AB at 3 dpf (Fig. S1 of the Supplementary Material). At 4 dpf, a much bigger difference between these strains is seen in the light-ON mean plots than the light-OFF ones (Fig. S1 of the Supplementary Material). Starting from 5 dpf onwards, the classification accuracies between the light-ON and light-OFF became comparable, with the accuracies for the light-ON stimulus being slightly higher.

4. Discussion

Different strains of WT zebrafish display different behaviours [43]. When their larvae are used in high-content behavioural studies, the variation in their behaviours [13,18,19] can affect the resulting interpretations. Among the high-content behavioural assays, use of the LLR has become very popular. However, most of the studies that utilised LLR analysed the data by binning the activities in mins. This approach does not permit the analysis of critical visual input that takes place during the first few seconds. For the few studies that analysed the data by binning the activities in seconds (i.e. utilising VMR), none studied the differences between WT strains. In this paper, we binned the data in seconds,

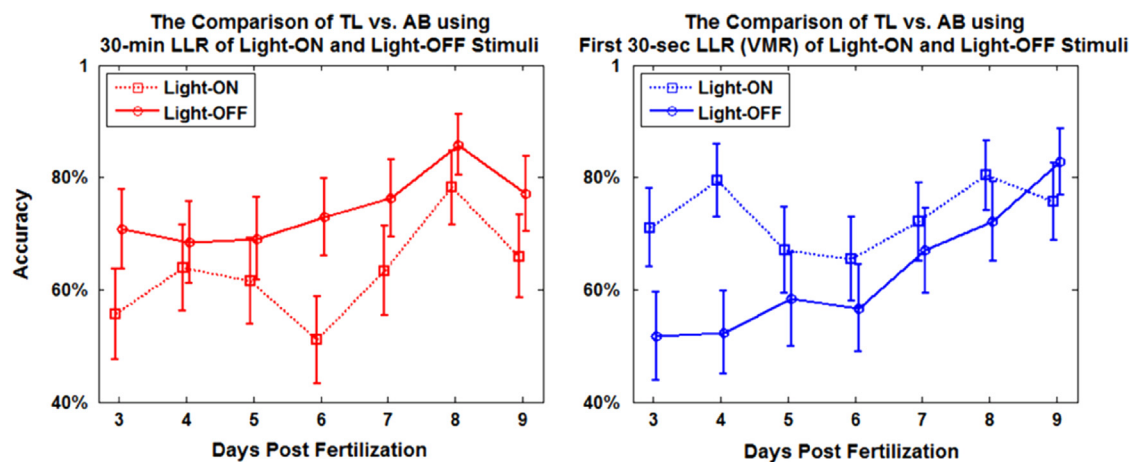


Fig. 5. Classification accuracies for TL vs. AB from 3 to 9 dpf using light-ON and light-OFF LLR data of different lengths. The left figure shows the classification results using the 30-min LLR data, while the right figure shows the results using the 30-s LLR (VMR) data. In each figure, the light-ON and light-OFF results were shown by the dotted line and solid line respectively. The line plots and the error bars indicate the mean and the standard deviation of the 500 times 10-fold cross validation.

and determined the difference between the complete 30-min LLR and its first 30-s subset (VMR) between three WT strains: AB, TL and TLAB. They were compared during early development from 3 to 9 dpf. The observations are summarised below.

First, the LLR varies between different WT strains at different stages (Fig. 2 and Fig. S1–S7 of the Supplementary Material), so that they can be moderately distinguished when compared pairwise (Fig. 3). In general, the change in classification accuracies during development has no clear pattern or trend. Nonetheless, the classification accuracies for TL vs. AB, when using the first 30-s LLR (VMR) data, were higher than the comparisons with TLAB. Since TLAB is a hybrid of TL and AB, its behaviour may have aspects in common with both; whereas the behaviours of TL and AB may be more distinct from each other. The relatively higher accuracies when classifying TL vs. AB obtained on 8 and 9 dpf implies that there were some major differences in locomotor behaviour development between TL and AB, particularly at later stages.

Second, our analysis revealed differences in the behaviour of AB and TL when using just the first 30-s LLR (VMR) data. While the difference in the longer-scale LLR between TL and AB was first observed by de Esch and colleagues [13], in their study, the LLR data were summarised in terms of minutes. While in our study, the data were summarised in seconds. This is the first demonstration that the short-term behavioural dynamics can be different between different WT strains. This finding is corroborated by the fact that using the first 30-s LLR (VMR) yielded superior accuracies compared with using the 30-min LLR for all stages except for 5 dpf (Fig. 4). Furthermore, the highest accuracy achieved in this study (90.6% for TL vs. AB at 8 dpf) was obtained using the first 30-s LLR (VMR) data. Thus, the VMR can provide desirable discriminatory power for behavioural changes because the most distinguishable information was detected immediately after the light change. This difference in the acute response (the first 30-s LLR [VMR]) of the WT strains implies a difference in their vision or locomotor circuitry, which would be distinct from the one that drives the long-term response (the 30-min LLR).

Third, the higher classification accuracy obtained in light-OFF stimulus suggests that three WT strains displayed a larger difference under the light-OFF stimulus than under the light-ON stimulus (Fig. 5). As larvae had a higher activity after light offset, the light-OFF classification accuracies were higher than the light-ON ones. This was true at all developmental stages tested when using a longer dataset (the 30-min LLR). A reverse trend was observed when a shorter dataset (the first 30-s LLR [VMR]) was used. This is probably due to

latter dataset measured a longer time span and captured extra speed-of-habituation information [25] that would only be apparent in minutes. Nonetheless, the classification accuracies in either light-ON or light-OFF stimulus are lower than that when both stimuli are combined (Fig. 4). Therefore, we recommend combining both light-ON and light-OFF data to achieve the best classification accuracy.

Several recent studies have begun to reveal the neural circuitry for the acute response (the first 30-s LLR [VMR]) and long-term response (the 30-min LLR), and for the light-ON and light-OFF response. Farida and colleagues first described eye function was essential for the acute response [23]. In particular, an eyeless *chokh/rx3* mutant did not display a VMR. By collecting VMR data in the same way (i.e. per second), we showed that the first 30-s LLR (VMR) was different from the long-term response (the 30-min LLR) in WT, strongly implying that the eye function substantially contributes to the first 30-s LLR (VMR). Interestingly, the same *chokh* mutant showed a slow light-OFF response that was apparent in minutes, when the behavioural data were colated into bins of minutes [26]. The authors revealed that pineal gland and a small region of hypothalamus perceived light offset, and contributed to this slow light-OFF response. Compared with the light-OFF response, less is known about the light-ON response. Nonetheless, both responses belong to the classical visual startle response in teleost fish [30,44] that can be triggered by rapid light onset and offset [45], or a looming stimulus [44,46, 47]. Thus, the current knowledge of startle response may give us further insights into the neural basis of different components of the VMR/LLR.

It has long been known that vibration-triggered startle response is initiated by a specific pair of Mauthner (M) cells in the hindbrain [44,48,49]. M-cell axon projects to the contralateral spinal cord, and innervates the primary motoneurons by direct and indirect connection [50–52]. As the M-cells receive visual inputs [53,54], these cells may drive the VMR. However, two recent studies have shown that the M-cells may not drive the critical part of the light-OFF VMR. In one of these studies, Burgess and Granato used a high-speed camera (in millisecond resolution) to capture the startle response after a dark flash [45]. They observed a new initial locomotor response from the larvae that they termed O-bend, in which the larvae twisted the body to form a circular shape. This O-bend is distinct from a less drastic version of body twisting called the C-bend/C-start response, which is long known to be initiated by the M-cells [44]. In fact, when the M-cells were ablated, the larvae still display an intact O-bend after the dark flash [45]. Interestingly, the O-bend is abolished after eye enucleation, suggesting that this locomotor response is initiated by retina

[26]. Therefore, it is likely that a different brain circuitry mediates this retinal-initiated O-bend, even though M-cells may drive different parts of the VMR/LLR. A possible candidate of this brain circuitry is the larger pool of reticulospinal neurons including M-cells [55] in the brainstem escape network (BEN) [50,51,56]. These neurons have been shown to control different parts of the escape response [57,58]. Thus, these neurons may control different parts of the VMR/LLR.

Our ongoing work will determine the details of visual inputs to the VMR/LLR, while future work should also focus on pinpointing the responsible circuit in the BEN that drives the response, and the genetic variations between the WT strains that caused the observed difference in their behavioural output. Before then, as different WT strains behave differently, VMR/LLR data obtained from one strain should be interpreted and generalised with care.

5. Conclusion

In summary, our investigation has used SVM to show that different WT larvae display different LLR. The SVM analyses also indicate that the distinguishable information in the VMR is comparable to, if not better than, the full LLR dataset for classification purposes. Furthermore, the distinguishable information of WT strains in the light-onset response differs from that in the light-offset response. While the classification accuracies were higher for the light-offset than light-onset response when using the complete LLR dataset, a reverse trend was observed when using a shorter VMR dataset. These behavioural differences are likely caused by differences in the neural circuitry and/or visual inputs. Our ongoing work will determine the details of visual inputs to the VMR/LLR, while future work should also focus on pinpointing the responsible circuit in the BEN that drives the response, and the genetic variations between the WT strains that caused the observed difference in their behavioural output. Before then, as different WT strains behave differently, VMR/LLR data obtained from one strain should be interpreted and generalised with care.

Conflict of interest

None declared.

Q5 Uncited reference

[28].

Acknowledgements

The work described in this paper was substantially supported by a Grant from the Research Grants Council of the Hong Kong Special Administrative Region, China (Project no. CityU 123312) and a Grant from City University of Hong Kong (Project no. 7200275). G. Zhang was partially supported by a William H. Phillips Summer Research Internship from Purdue University. R. Carmer was partially supported by a Howard Hughes Medical Institute Undergraduate Research Experience Program from Purdue University. P. Venkatraman was partially supported by a Faculty for the Future Fellowship by the Schlumberger Foundation. C.P. Pang was partially supported by a Direct Grant (Grant no. 2041771) from the Medical Panel, The Chinese University of Hong Kong, and a General Research Fund (Grant no. 2140694) from the Research Grants Council of Hong Kong. M. Zhang was partially supported by the National Scientific Foundation of China (Grant no. 81486126),

the Provincial Natural Scientific Foundation of China (Grant no. 8151503102000019), and the Ministry of Health Program of Public Welfare (Grant no. 201302015).

Appendix A. Supplementary material

Supplementary data associated with this article can be found in the online version at <http://dx.doi.org/10.1016/j.combiomed.2015.11.012>.

References

- [1] G.J. Lieschke, P.D. Currie, Animal models of human disease: zebrafish swim into view, *Nat. Rev. Genet.* 8 (2007) 353–367.
- [2] E.E. Patton, L.I. Zon, The art and design of genetic screens: zebrafish, *Nat. Rev. Genet.* 2 (2011) 956–966.
- [3] J.D. Best, W.K. Alderton, Zebrafish: an in vivo model for the study of neurological diseases, *Neuropsychiatr. Dis. Treat.* 4 (2008) 567–576.
- [4] D. Kokel, et al., Rapid behavior-based identification of neuroactive small molecules in the zebrafish, *Nat. Chem. Biol.* 6 (2010) 231–237.
- [5] D.A. Prober, et al., Hypocretin/orexin overexpression induces an insomnia-like phenotype in zebrafish, *J. Neurosci.* 26 (2006) 13400–13410.
- [6] J. Rihel, et al., Zebrafish behavioral profiling links drugs to biological targets and rest/wake regulation, *Science* 327 (2010) 348–351.
- [7] L. Yu, et al., Cognitive aging in zebrafish, *Plos One* 1 (2006) e14.
- [8] I.V. Zhdanova, et al., Aging of the circadian system in zebrafish and the effects of melatonin on sleep and cognitive performance, *Brain Res. Bull.* 75 (2008) 433–441.
- [9] J. Rihel, A.F. Schier, Behavioral screening for neuroactive drugs in zebrafish, *Dev. Neurobiol.* 72 (2012) 373–385.
- [10] S. Ali, et al., Large-scale analysis of acute ethanol exposure in zebrafish development: a critical time window and resilience, *Plos One* 6 (2011) e20037.
- [11] S. Ali, D.L. Champagne, M.K. Richardson, Behavioral profiling of zebrafish embryos exposed to a panel of 60 water-soluble compounds, *Behav. Brain Res.* 228 (2012) 272–283.
- [12] S. Deeti, S. O'Farrell, B.N. Kennedy, Early safety assessment of human oculo-toxic drugs using the zebrafish visualmotor response, *J. Pharmacol. Toxicol. Methods* 69 (2014) 1–8.
- [13] C. de Esch, et al., Locomotor activity assay in zebrafish larvae: influence of age, strain and ethanol, *Neurotoxicol. Teratol.* 34 (2012) 425–433.
- [14] R.C. MacPhail, et al., Locomotion in larval zebrafish: influence of time of day, lighting and ethanol, *Neurotoxicology* 30 (2009) 52–58.
- [15] L. Zhang L, et al., Drug screening to treat early-onset eye diseases: can zebrafish expedite the discovery? *Asia-Pac. J. Ophthalmol.* 1 (2012) 374–383.
- [16] K.H. Brown, et al., Extensive genetic diversity and substructuring among zebrafish strains revealed through copy number variant analysis, *Proc. Natl. Acad. Sci.* 109 (2012) 529–534.
- [17] T.S. Coe, et al., Genetic variation in strains of zebrafish (*Danio rerio*) and the implications for ecotoxicology studies, *Ecotoxicology* 18 (2009) 144–150.
- [18] M. Lange, et al., Inter-individual and inter-strain variations in zebrafish locomotor ontogeny, *Plos One* 8 (2013) e70172.
- [19] C. Vignet, et al., Systematic screening of behavioral responses in two zebrafish strains, *Zebrafish* 10 (2013) 365–375.
- [20] S. Mahabir, et al., Maturation of shoaling in two zebrafish strains: a behavioral and neurochemical analysis, *Behav. Brain Res.* 247 (2013) 1–8.
- [21] S. Padilla, et al., Assessing locomotor activity in larval zebrafish: influence of extrinsic and intrinsic variables, *Neurotoxicol. Teratol.* 33 (2011) 624–630.
- [22] Y. Gao, et al., A high-throughput zebrafish screening method for visual mutants by light-induced locomotor response, *IEEE/ACM Trans. Comput. Biol. Bioinf.* 11 (2014) 693–701.
- [23] F. Emran, et al., OFF ganglion cells cannot drive the optokinetic reflex in zebrafish, *Proc. Natl. Acad. Sci.* 104 (2007) 19126–19131.
- [24] C.M. Maurer, et al., Distinct retinal deficits in a zebrafish pyruvate dehydrogenase-deficient mutant, *J. Neurosci.* 30 (2010) 11962–11972.
- [25] A. Bekker van Woudenberg, et al., A category approach to predicting the developmental (neuro) toxicity of organotin compounds: the value of the zebrafish (*Danio rerio*) embryotoxicity test (ZET), *Reprod. Toxicol.* 41 (2013) 35–44.
- [26] A.M. Fernandes, et al., Deep brain photoreceptors control light-seeking behavior in zebrafish larvae, *Curr. Biol.* 22 (2012) 2042–2047.
- [27] F. Emran, J. Rihel, A.E. Dowling, A behavioral assay to measure responsiveness of zebrafish to changes in light intensities, *J. Vis. Exp.* 20 (2008) 1–6.
- [28] A. Franke, T. Caelli, R.J. Hudson, Analysis of movements and behavior of caribou (*Rangifer tarandus*) using hidden Markov models, *Ecol. Model.* 173 (2–3) (2004) 259–270.
- [29] Y. Liu, S.-H. Lee, T.-S. Chon, Analysis of behavioral changes of zebrafish (*Danio rerio*) in response to formaldehyde using self-organizing map and a hidden Markov model, *Ecol. Model.* vol. 222 (no. 14) (2011) 2191–2201.

- [30] Y. Li, J.-M. Lee, T.-S. Chon, Y. Liu, H. Kim, M.-J. Bae, Y.-S. Park, Analysis of movement behavior of zebrafish (*Danio rerio*) under chemical stress using hidden Markov model, *Mod. Phys. Lett. B* 27 (2) (2013) 1350014:1–1350014:13.
- [31] O. Mirat, J.R. Sternberg, K.E. Severi, C. Wyart, ZebraZoom: an automated program for high-throughput behavior analysis and categorization, *Front. Neural Circuits* 7 (2013) 107:1–107:12.
- [32] R. Liu, et al., Automated phenotype recognition for zebrafish embryo based in vivo high throughput toxicity screening of engineered nano-materials, *Plos One* 7 (2012) e35014.
- [33] M.R. Hensley, Y.F. Leung, A convenient dry feed for raising zebrafish larvae, *Zebrafish* 7 (2010) 219–231.
- [34] Y. Liu, et al., Statistical analysis of zebrafish locomotor response, *Plos One* 10 (2015) e0139521.
- [35] S.S. Easter Jr., G.N. Nicola, The development of vision in the zebrafish (*Danio rerio*), *Dev. Biol.* 180 (1996) 646–663.
- [36] S.S. Easter Jr., G.N. Nicola, The development of eye movements in the zebrafish (*Danio rerio*), *Dev. Psychobiol.* 31 (1997) 267–276.
- [37] J.M. Fadool, J.E. Dowling, Zebrafish: a model system for the study of eye genetics, *Prog. Retin. Eye Res.* 27 (2008) 89–110.
- [38] J. Lin, et al., Experiencing SAX: a novel symbolic representation of time series, *Data Min. Knowl. Discov.* 15 (2007) 107–144.
- [39] J.S. Richman, J.R. Moorman, Physiological time-series analysis using approximate entropy and sample entropy, *Am. J. Physiol. Heart Circ. Physiol.* 278 (2000) H2039–H2049.
- [40] C.D. Cantrell, *Modern Mathematical Methods for Physicists and Engineers*, Cambridge University Press, 2000.
- [41] C.C. Chang, C.J. Lin, LIBSVM: a library for support vector machines, *ACM Trans. Intell. Syst. Technol.* 2 (2011) 1–27.
- [42] G. Seni, J.F. Elder, *Ensemble Methods in Data Mining: Improving Accuracy Through Combining Predictions*, Morgan and Claypool Publishers, 2010.
- [43] W. Norton, L. Bally-Cuif, Adult zebrafish as a model organism for behavioural genetics, *BMC Neurosci.* 11 (2010) 90.
- [44] R.C. Eaton, R.A. Bombardieri, D.L. Meyer, The Mauthner-initiated startle response in teleost fish, *J. Exp. Biol.* 66 (1977) 65–81.
- [45] H.A. Burgess, M. Granato, Modulation of locomotor activity in larval zebrafish during light adaptation, *J. Exp. Biol.* 210 (2007) 2526–2539.
- [46] T. Preuss, et al., Neural representation of object approach in a decision-making motor circuit, *J. Neurosci.* 26 (2006) 3454–3464.
- [47] S.A. Weiss, et al., Correlation of C-start behaviors with neural activity recorded from the hindbrain in free-swimming goldfish (*Carassius auratus*), *J. Exp. Biol.* 209 (2006) 4788–4801.
- [48] R.C. Eaton, et al., Functional development in the Mauthner cell system of embryos and larvae of the zebra fish, *J. Neurobiol.* 8 (1977) 151–172.
- [49] C.B. Kimmel, J. Patterson, R.O. Kimmel, The development and behavioural characteristics of the startle response in the zebra fish, *Dev. Psychobiol.* 7 (1974) 47–60.
- [50] R.C. Eaton, R.K. Lee, M.B. Foreman, The Mauthner cell and other identified neurons of the brainstem escape network of fish, *Prog. Neurobiol.* 63 (2001) 467–485.
- [51] V. Medan, T. Preuss, The Mauthner-cell circuit of fish as a model system for startle plasticity, *J. Physiol. Paris* 108 (2014) 129–140.
- [52] S.J. Zottoli, D.S. Faber, The Mauthner cell: what has it taught us? *The Neuroscientist* 6 (2000) 26–38.
- [53] S.J. Zottoli, A.R. Hordes, D.S. Faber, Localization of optic tectal input to the ventral dendrite of the goldfish Mauthner cell, *Brain Res.* 401 (1987) 113–121.
- [54] S.J. Zottoli, et al., Comparative studies on the Mauthner cell of teleost fish in relation to sensory input, *Brain Behav. Evol.* 46 (1995) 151–164.
- [55] C.B. Kimmel, S.L. Powell, W.K. Metcalfe, Brain neurons which project to the spinal cord in young larvae of the zebrafish, *J. Comp. Neurol.* 205 (1982) 112–127.
- [56] J.G. Canfield, Functional evidence for visuospatial coding in the Mauthner neuron, *Brain Behav. Evol.* 67 (2006) 188–202.
- [57] F.A. Issa, et al., Neural circuit activity in freely behaving zebrafish (*Danio rerio*), *J. Exp. Biol.* 214 (2011) 1028–1038.
- [58] T. Kohashi, Y. Oda, Initiation of Mauthner- or non-Mauthner-mediated fast escape evoked by different modes of sensory input, *J. Neurosci.* 28 (2008) 10641–10653.

Yuan Gao received the BS degree in biomedical engineering in 2009 and the MS degree in pattern recognition and intelligent systems in 2012, both from Huazhong University of Science and Technology. He is currently working toward the Ph.D. degree in the Department of Electronic Engineering, City University of Hong Kong. His research interests include machine learning, pattern recognition, and applications.

Gaonan Zhang was an undergraduate student researcher in the Department of Biological Sciences at Purdue University. He is currently a Ph.D. student in the PULSe program at Purdue University.

Beth Jeffs is a Research Fellow in the Laboratory for Computational Neuroscience, Department of Electronic Engineering at City University of Hong Kong. She graduated from the University of Leicester, UK with a MEng (1st Hons.) in Electronic & Software Engineering, receiving the British Computer Society prize for top graduate 2005, and from Imperial College London with a Ph.D. in Electrical and Electronic Engineering in 2010. She has previously held post-doctoral research positions in the Biomedical Optics Research Laboratory, Department of Medical Physics & Bioengineering at University College London, UK and the Bayley Group, Department of Chemistry at the University of Oxford, UK. She was on the organising committee of the enGENEious conference on synthetic biology and microbial engineering, 2012 and an event manager for the Pint of Science festival, 2013. Her current research interests include statistical and adaptive signal processing, machine learning and signal modality characterisation and in particular their application to biomedical data.

Robert Carmer was an undergraduate student researcher in the Department of Biological Sciences at Purdue University.

Prahatha Venkatraman received her B. Tech degree from SASTRA University in Thanjavur, India. She is currently a Ph.D. student in the Department of Biological Sciences at Purdue University, and a Schlumberger Foundation Faculty for Future Fellow.

Mohammad Ghadami received the BS degree in Mechanical Engineering from K.N. Toosi University of Technology in 2009 and MS degree in Mechatronics Engineering from University of Tehran, Iran, in 2012. He was a RA in the Department of Electronic Engineering at City University of Hong Kong in 2013.

Skye Brown is a technician in the Department of Biological Sciences at Purdue University.

Calvin C.P. Pang is S.H. Ho Professor of Visual Sciences, Professor of Ophthalmology and Visual Sciences, and Chairman at the Department of Ophthalmology and Visual Sciences at The Chinese University of Hong Kong. He is also Director of The Shantou University / The Chinese University of Hong Kong Joint Shantou International Eye Centre. His research interests include genomic studies and gene mapping of glaucoma, retinal diseases, myopia, congenital cataracts, retinoblastoma, thyroid-associated orbitopathy, diabetic retinopathy, retinitis pigmentosa, uveitis, and corneal dystrophies. He also works on ocular stem cells and herbal molecules on their effects in eye diseases. Prof. Pang received a BSc in Biochemistry in 1978 from the University of London and DPhil in 1982 at the University of Oxford on an EP Abraham Research Fund Scholarship, followed by two years' postdoctoral research in Oxford. Prof. Pang has more than 310 publications and 13 book chapters. He is a reviewer for the Wellcome Trust (UK), National Eye Institute (USA), National Medical Research Council (Singapore), Health Research Board (Ireland), Catalan Agency for Health Technology Assessment and Research (Spain), and National Science Foundation China. He is honorary or visiting professor of more than 20 clinical or research institutions in mainland China.

Yuk Fai Leung is an Associate Professor in the Department of Biological Sciences at Purdue University. He received a B.Sc. (1st Hon.) degree and an M.Phil. degree in Biochemistry from the Hong Kong University of Science and Technology in 1996 and 1998 respectively. He received his Ph.D. degree in Ophthalmology from the Chinese University of Hong Kong in 2002. Dr. Leung was awarded with a Croucher Foundation Postdoctoral Fellowship the same year and pursued his postdoctoral research at Harvard University until 2007. In 2005, he was awarded with a Paediatric Ophthalmology Research Grant from the Knights Templar Eye Foundation. In 2008, Dr. Leung established his own research group at Purdue University in the Department of Biological Sciences. He also received a Hope for Vision Award in the same year. His current research focuses on using zebrafish eye disease models to elucidate disease-causing gene network and identify new drug therapies.

Rosa H.M. Chan received the B.Eng (1st Hon.) degree in Automation and Computer-Aided Engineering and a minor in Computer Science from the Chinese University of Hong Kong in 2003. She was later awarded the Croucher Scholarship and Sir Edward Youde Memorial Fellowship for Overseas Studies in 2004. In the summer of 2010, she was awarded Google Scholarship and participated in the Singularity University Graduate Studies Program at NASA AMES. She received her Ph.D. degree in Biomedical Engineering in 2011 at University of Southern California (USC), where she also received her M.S. degrees in Biomedical Engineering, Electrical Engineering, and Aerospace Engineering. Dr. Chan is currently an Assistant Professor in the Department of Electronic Engineering at City University of Hong Kong. Her research interests include mathematical modeling of neural system, development of neural prosthesis, and brain-machine interface applications.

Zhang Mingzhi has been working on Ophthalmology for more than 30 years, with subspecialty in Cataract, Glaucoma and Optometry. She is the pioneer of phacemulsification and refractive surgery for cataract. Her study of surgical treatment of glaucoma with cataract has attracted great attention in these fields. Recently by combining both basic research and clinical research together, she focused on mapping of disease causing genes of congenital cataract as well as susceptibility genes of glaucoma and high myopia. She has conducted 6 research projects founded national wide, 2 International cross-cutting projects, 3 provincial research projects in recent years. 131 papers have been published in national and provincial journals, of which there are 61 papers accepted in international peer reviewed SCI journals.

UNCORRECTED PROOF